Global modeling analysis of tropospheric ozone and its radiative forcing from biomass burning emissions in the twentieth century

Akinori Ito,[1] Kengo Sudo,[1] Hajime Akimoto,[1] Sanford Sillman,[2] and Joyce E. Penner[2]

Received 3 April 2007; revised 18 June 2007; accepted 24 September 2007; published 29 December 2007.

[1] This work evaluates the sensitivity of tropospheric ozone (O_3) and its radiative forcing (RF) from 1890 to 1990 to different biomass burning (BB) emissions using a global tropospheric climate-chemistry model (CCM) with a modified chemical mechanism for anthropogenic volatile organic compounds (AVOC). The use of the most efficient simplified chemical scheme among three chemical mechanisms with different degrees of complexity is acceptable for global scale simulations of the radiative effects of tropospheric O_3 changes in the CCM, since the differences in the results are small. The CCM model with simplified chemistry is implemented to study various aspects of the impact of BB emissions on tropospheric O_3 and its RF. The backward emission model results are in good agreement with the present-day observations for regions downwind of BB sources, while the forward emission model may reasonably produce the distributions of regional emissions in the preindustrial period. The global mean RF due to tropospheric O_3 increase from 1890 to 1990 is 0.41 W m^{-2} on a global average. When no anthropogenic emissions in the preindustrial period are considered, this forcing reaches 0.47 W m^{-2}. We find that the global mean BB forcing due to tropospheric O_3 changes from 1890 to 1990 is 0.15 W m^{-2} on a global average. The preindustrial BB emissions need to be represented realistically when evaluating controls on the emissions of trace gases and aerosols for a sustainable society, because there are significant open biomass burning emissions in the preindustrial period. The significant regional differences in the surface O_3 concentrations among three different BB data sets are found in the United States for 1890 and in Brazil for 1990. In these regions during the periods, the most common land uses in the forests are logging and conversion of primary or secondary forests to cattle pasture or shifting cultivation. Improvement in the data sets of historical land use changes and accurate representation of carbon dynamics are needed for improving the model calculation of biomass burning emissions.

Citation: Ito, A., K. Sudo, H. Akimoto, S. Sillman, and J. E. Penner (2007), Global modeling analysis of tropospheric ozone and its radiative forcing from biomass burning emissions in the twentieth century, *J. Geophys. Res.*, *112*, D24307, doi:10.1029/2007JD008745.

1. Introduction

[2] Biomass burning (BB) is one of the most significant sources of trace gases and aerosols on a global scale [*Crutzen et al.*, 1979; *Logan et al.*, 1981; *Andreae and Crutzen*, 1997]. The influence of BB emissions on tropospheric ozone (O_3) has been investigated in numerous measurements and modeling studies [*Crutzen and Zimmermann*, 1991; *Thompson et al.*, 2001; *Swap et al.*, 2003; *Fehsenfeld et al.*, 2006]. Recently, three historical emission data sets from *van Aardenne et al.* [2001], *Ito and Penner* [2005a], and *Mouillot et al.* [2006] have indicated that there are significant preindustrial emissions from open biomass burning. The database of *van Aardenne et al.* [2001] has been compared to the conventional assumption (i.e., zero anthropogenic emissions and 10% open biomass burning emissions from their present-day estimates for the preindustrial simulations [*Crutzen and Zimmermann*, 1991]) by *Lamarque et al.* [2005]. They found that from 1890 to 1990 the tropospheric O_3 burden increased by only 71 Tg with the *van Aardenne et al.* [2001] inventory compared to an increase of 88 Tg with the conventional assumption. The van Ardenne et al. database has been used for the estimates of the contribution of tropospheric O_3 changes to recent climate trends by *Shindell et al.* [2006]. They estimated a total instantaneous forcing of 0.41 W m^{-2} and an adjusted forcing (which allows stratospheric temperature to respond to the forcing) of 0.34 W m^{-2}.

[3] Sensitivity studies have shown the importance of regional O_3 changes on RF in areas where there have been strong increases in the emissions of O_3 precursors [e.g., *Fuglestvedt et al.*, 1999; *Berntsen et al.*, 2005; *Naik et al.*,

[1] Frontier Research Center for Global Change, Japan Agency for Marine-Earth Science and Technology, Yokohama, Japan.
[2] Department of Atmospheric, Oceanic and Space Sciences, University of Michigan, Ann Arbor, Michigan, USA.

0148-0227/07/2007JD008745

Table 1. Summary of Different Simulations Performed in This Study

Name	Chemical Mechanism	Emission Database	Seasonal Variation
CM1-ED1-SV1	*Sudo et al.* [2002a]	*van Aardenne et al.* [2001]	*Arino and Plummer* [2001]
CM2-ED1-SV1	*Ito et al.* [2007b]	*van Aardenne et al.* [2001]	*Arino and Plummer* [2001]
CM3-ED1-SV1	this work	*van Aardenne et al.* [2001]	*Arino and Plummer* [2001]
CM3-ED2-SV1	this work	*Ito and Penner* [2005a]	*Arino and Plummer* [2001]
CM3-ED3-SV1	this work	*Mouillot et al.* [2006]	*Arino and Plummer* [2001]
CM3-ED4-SV1	this work	*Crutzen and Zimmermann* [1991]	*Arino and Plummer* [2001]
CM3-ED2-SV2	this work	*Ito and Penner* [2005a]	*Herman et al.* [1997]
CM3-ED2-SV3	this work	*Ito and Penner* [2005a]	*Giglio et al.* [2006]
CM3-BB-1890	this work	*van Aardenne et al.* [2001]	*Arino and Plummer* [2001]
CM3-FF-1890	this work	*van Aardenne et al.* [2001]	–

2005]. *Naik et al.* [2007] investigated the sensitivity of direct RF due to tropospheric O_3 and carbonaceous and sulfate aerosols to a 10% reduction in the emissions from major BB regions. They found a global RF of -4.1 mW m^{-2} from tropospheric O_3 and -4.1 mW m^{-2} from aerosols for Africa and -3.0 mW m^{-2} from tropospheric O_3 and -2.8 mW m^{-2} from aerosols for South America. The estimates for forcing due to BB aerosol is expected to have a high uncertainty just due to present-day estimates of the emissions [e.g., *Ito and Penner*, 2005b; *Andreae and Gelencser*, 2006], but *Textor et al.* [2007] found that the simulated aerosol burden and optical properties depend more on the model-specific transport, removal, chemistry, and parameterizations of aerosol microphysics rather than on the spatial and temporal distributions of the emissions. However, differences in different emission databases need to be considered when evaluating the impact of BB to improve modeling studies.

[4] The uncertainties in the BB emissions are also associated with the seasonal variations. *Schultz* [2003] used fire products from the Along Track Scanning Radiometer (ATSR) satellites to analyze spatial and temporal variations in emissions from BB. The bias in active fire products is significantly large without a quantitative validation and calibration using high-resolution data [e.g., *Kasischke et al.*, 2003; *Boschetti et al.*, 2004]. Further, seasonal variations in the emissions are substantially influenced by the available biomass for combustion (i.e., fuel load) and burning conditions (i.e., flaming and smoldering fires) [e.g., *Hoffa et al.*, 1999; *Bertschi et al.*, 2003; *Korontzi et al.*, 2003]. *Duncan et al.* [2003] made use of the Total Ozone Mapping Spectrometer (TOMS) Aerosol Index (AI) data product as a surrogate to estimate seasonal and interannual variability in BB. The interannual variability of O_3 produced by BB is important in southeastern Asia [e.g., *Page et al.*, 2002; *van der Werf et al.*, 2004].

[5] Integrating a complicated photochemical scheme into a global climate model increases the CPU time needed for calculations. Fast chemical solution methods are useful in investigating the factors affecting the O_3 changes, because the chemistry is often the most time consuming part of the calculations. Also, the total number of primary pollutants and their reaction products are often simplified in global CTMs and CCMs [e.g., *Müller and Brasseur*, 1995; *Houweling et al.*, 1998; *Shindell et al.*, 2003; *Wong et al.*, 2004]. To increase the accuracy and reduce the uncertainty in the models, it is essential that the simplified model provide results that are equivalent to more complete chemical mechanisms.

[6] The purpose of this paper is to investigate the effects of different BB emission changes on tropospheric O_3. For this purpose, a coupled chemistry-climate model with a fast chemical mechanism for anthropogenic volatile organic compounds (AVOC) is used to calculate the O_3 concentration and its RF. Section 2 describes the CCM used for estimating the differences in the chemical mechanisms for AVOC and emission estimates. Section 3 describes the different emission data sets for BB sources. Section 4 shows an evaluation of the representation for AVOC on tropospheric O_3 as well as the sensitivity of the O_3 concentration and its RF to different BB emissions. We also show comparisons with O_3 observations for regions downwind of BB sources. Section 5 presents a summary of our findings.

2. Model Description

[7] We investigate the effects of different AVOC chemical mechanisms and BB emissions on tropospheric O_3 and its RF using the Chemical Atmospheric general circulation model for the Study of the atmospheric Environment and Radiative forcing (CHASER) model [*Sudo et al.*, 2002a; *Sudo and Akimoto*, 2007], which has been applied in the integrated earth system model [*Kawamiya et al.*, 2005], with an online simulation of gas-phase chemistry [*Sudo et al.*, 2002a] and aerosols [*Takemura et al.*, 2000]. The different simulations performed in this study are summarized in Table 1. Our two-way coupling between aerosols and gas-phase chemistry provides consistent chemical fields for aerosol dynamics and aerosol mass for heterogeneous processes and calculations of gas-phase photolysis rates [e.g., *Liao et al.*, 2003].

[8] To evaluate the impact of the modeled tropospheric O_3 changes on climate, we use the RF calculated from the CCM simulations. The instantaneous shortwave and longwave radiative fluxes at the tropopause were calculated by the k-distribution and the two-stream discrete ordinate method [*Nakajima and Tanaka*, 1986]. Absorption and scattering were calculated for gases, aerosols, and clouds. For a complete description of the radiation scheme adopted in the model, the reader is referred to *Nakajima et al.* [1995, and references therein].

[9] Two separate simulations are performed for calculations of radiative fluxes for 1890 and 1990, respectively [e.g., *Shindell et al.*, 2003]. The differences in the radiative fluxes are calculated for 1890 and 1990 by calling the radiation code twice, once based on the climatologically

simulated O_3 archived daily in previous work [*Sudo et al.*, 2002a] and once based on the inline calculated distribution in this work. Then the RF is calculated from the differences in the radiative fluxes at the tropopause between the 1890 and 1990 simulations. The tropopause height is defined as the lowest level at which the vertical temperature gradient is greater than -2 K km^{-1} [e.g., *Logan*, 1999]. The adjusted forcing is more indicative of the climate impacts of tropospheric O_3 changes [*Hansen et al.*, 2002], however, the instantaneous forcing is used here to examine the sensitivity to different sources [e.g., *Shindell et al.*, 2006].

[10] In these simulations, we used meteorological fields of wind velocities and temperature from the European Center for Medium-Range Weather Forecasts (ECMWF) to constrain the dynamic component of the model, in addition to sea surface temperature data for 1996. This ensures that the effects of different AVOC chemical mechanisms and BB emissions on tropospheric O_3 are separated from the climate feedback. The meteorology was defined on about 2.8° latitude × 2.8° longitude horizontal grid (T42) with 32 vertical sigma layers. The evolution of species was calculated with a time step of 10 min. The model was exercised for a 1-year time period with 6-month spin-up time.

[11] Three different chemical mechanisms with different degrees of complexity were examined to quantify the differences due to different AVOC chemical representations and to determine the standard chemistry for later simulations in this paper. The default chemical mechanism (CM1) in the model is described by *Sudo et al.* [2002a]. It includes 38 tracers, 12 short-lived compounds that are not transported, and 141 reactions. The photochemical representation for AVOC is based on the IMAGES chemical mechanism [*Müller and Brasseur*, 1995] and the MOZART model [*Brasseur et al.*, 1998], and uses a lumped compound, other nonmethane volatile organic compounds (ONMV), as a surrogate for the NMVOC (i.e., C_2H_6, C_3H_8, C_2H_4, and C_3H_6). The ONMV + OH-reaction rate constant at 298 K was taken from the average OH-reaction rate of NMVOC weighted by their anthropogenic emissions [*Middleton et al.*, 1990]. The climatological simulation of the CHASER model with the similar chemical scheme to CM1 has been evaluated with several observational data sets by *Sudo et al.* [2002b]. Their evaluation showed that the model captured the geographic, vertical and seasonal variations of O_3 quite well. The calculated O_3 concentrations were also in good agreement with the ensemble mean when constraining precursor emissions [*Stevenson et al.*, 2006].

[12] *Ito et al.* [2007b] extended the photochemistry representation from the 3-D chemical transport model (GEOS-Chem) [*Bey et al.*, 2001]. The species that are emitted into the model atmosphere are specified with more explicit surrogates [*Ito et al.*, 2007b]. The recent mechanism of *Ito et al.* [2007b] includes detailed descriptions for a wider set of organic compounds than are typically included in global models and is termed the "extended" mechanism (CM2). The ONMV is specified as three primary aromatic species, two alkanes and one alkene, and their various secondary reaction products are treated. The extended mechanism includes 61 tracers, 56 nontracers, and 400 reactions. A complete listing of reactions is available at http://www-personal.umich.edu/~sillman/web-publications/Ito_2007_TableA1.pdf. *Ito et al.* [2007b] has evaluated the CM3 with several observations in the 3-D chemical transport model (IMPACT) model. They showed that the model-measurement agreement was as good as the chemical mechanism used in the GEOS-Chem model [*Bey et al.*, 2001].

[13] Given the need to conserve computational resources for a CCM [e.g., *Shindell et al.*, 2005, 2006], it is necessary to group organic compounds together to form the smallest possible set of model classes. In these "condensed" mechanisms (CM3) multiple chemical pathways are treated as one reaction, and not all organic intermediates (i.e., alkyl radicals) are explicitly described. Here, we formed a condensed mechanism (CM3) based on the grouping suggested by *Jacob et al.* [1989] from the extended chemical mechanism of *Ito et al.* [2007b]. They identified the most important features of individual AVOC as (1) the lifetime (hours versus days) and (2) the tendency of the compound to be a net producer of odd hydrogen radicals (OH, HO_2, and RO_2). The appropriate product yields and weighted averages of reaction rate constants were determined using the 0-d model developed by *Sillman* [1991] and were based on the number of species lumped in each group and their species concentrations (except for the isoprene and terpene chemistry, as noted below in this section). For further detail, the reader is referred to *Jacob et al.* [1989]. The four alkanes, benzene, toluene (as a surrogate for all alkylbenzenes), two ketones, acetic acid and larger organic acids in the extended chemistry of *Ito et al.* [2007b] are represented with a Slower Reacting Species (SRS), while three alkenes and m-xylene (as a surrogate for dialkyl- and trialkylbenzenes) are represented with a Faster Reacting Species (FRS). The condensed chemistry includes 26 tracers, 12 nontracers, and 137 reactions in the model.

[14] The chemical schemes for isoprene [*Pöschl et al.*, 2000] and terpenes [*Brasseur et al.*, 1998] in the default chemical mechanism are used in the extended and simplified chemical mechanisms as well. Here, we focus on the direct forcing from O_3 on climate, and ignore possible secondary effects such as impact on CH_4 through changed OH [e.g., *Wild and Prather*, 2000; *Dentener et al.*, 2005; *Dalsøren and Isaksen*, 2006; *Fiore et al.*, 2006]. The methane changes enhance the OH perturbation through a positive feedback, but this is not crucial for the short-lived mode perturbations performed here [e.g., *Wild and Prather*, 2000; *Wild et al.*, 2001]. Thus uniform mixing ratios for present-day CH_4 were set to 1.77 ppmv in the Northern Hemisphere (NH) and 1.68 ppmv in the Southern Hemisphere and to 0.70 ppmv for the preindustrial simulation on the basis of observations [*Etheridge et al.*, 1998; *Dlugokencky et al.*, 1998].

[15] For the base emission inventory, we use the data set of *van Aardenne et al.* [2001]. The 1° × 1° grid emissions are based on historical activity data and are available every 10 years from 1890 to 1990. We compare the base BB emission inventory to the conventional assumption [*Crutzen and Zimmermann*, 1991] and to more recent data sets [*Ito and Penner*, 2005a; *Mouillot et al.*, 2006], as described in section 3. The industrial emissions of *van Aardenne et al.* [2001] are the same in the three BB emission inventories. The default seasonal cycle in emissions is taken to be the same as that given by *Sudo et al.* [2002a]. To fit our set of

modeled chemical species, we have made the assumption that the 1990 speciation of the nonmethane hydrocarbon emissions [*Olivier et al.*, 1999] was valid for the entire period of this study. The black carbon emission data set for the time period from 1870 to 2000 is taken from *Ito and Penner* [2005a]. Other aerosol emissions are set as in the work by *Takemura et al.* [2000]. Thus the aerosols in the model are the same for all simulations.

[16] Natural emissions from vegetation, ocean, and soils for the preindustrial simulation are the same as for the present-day simulations. The biogenic emissions of NMVOC were based on *Guenther et al.* [1995]. The emissions for isoprene and terpenes were reduced by 20%, following *Houweling et al.* [1998] and *Roelofs and Lelieveld* [2000]. The diurnal cycle of isoprene emission was calculated using solar incidence at the surface, while that of terpenes was parameterized using surface air temperature in the model [*Guenther et al.*, 1995]. We also scaled the geographic distribution of ocean emissions of hydrocarbons [*Müller*, 1992] to the more recent estimates of *Plass-Dülmer et al.* [1995], following *von Kuhlmann et al.* [2003]. The soil NO_x emissions are taken from *van Aardenne et al.* [2001], which take into account the effect of increased fertilizer use.

3. Biomass Burning Emission Data Sets

[17] Here, we describe the present-day and preindustrial biomass burning emission data sets used in this study. We define biomass burning as savanna burning, forest fires, agricultural waste burning, and biomass used for fuels (biofuels). We examine four different data sets of BB emissions (ED1, ED2, ED3, and ED4) and three different seasonal variations (SV1, SV2, and SV3) with one of the data sets. Each data set provides emission estimates for 1890 and 1990.

[18] First (ED1), *van Aardenne et al.* [2001] used the present-day emissions of *Hao et al.* [1990] and *Bouwman et al.* [1997] from open biomass burning, assuming that all BB in the wet savanna was anthropogenic in origin while half was anthropogenic in the dry savanna. The ED1 used rural population as a surrogate for emissions from deforestation fires in tropical regions and neglected deforestation activities in industrialized regions. Thus the anthropogenic emissions from the BB due to land use changes for 1890 were projected by using present-day emissions [*Olivier et al.*, 1999] and adjusting on the basis of changes in rural population [*Klein Goldewijk*, 2001]. The ED1 present-day emissions from biofuel burning [*Olivier et al.*, 1999] were also extrapolated back in time using the rural population data. The ED1 used the amount of arable land as a proxy for historical agricultural waste burning. Thus the emissions from agricultural waste burning for 1890 were estimated by using present-day emissions [*Olivier et al.*, 1999] and adjusting on the basis of changes in arable land area [*Klein Goldewijk*, 2001].

[19] Second (ED2), we used the $1^\circ \times 1^\circ$ gridded data set of *Ito and Penner* [2005a]. The ED2 emissions from open biomass burning were based on present-day emissions estimates from the spatially resolved monthly emissions of *Ito and Penner* [2004] and the regionally constrained annual carbon monoxide (CO) emissions of *Arellano et al.* [2004] for open vegetation burning. The open vegetation burning emissions were extrapolated back in time for 1979–2000 using satellite data from the TOMS instrument [*Herman et al.*, 1997] and for 1870–1978 using anthropogenic CH_4 emissions from BB [*Stern and Kaufmann*, 1996]. *Stern and Kaufmann* [1996] based their BB emissions estimates on anthropogenic carbon dioxide emissions from land use change estimated by *Houghton et al.* [1983]. The ED2 present-day emissions from biofuel burning were calculated from *Food and Agricultural Organization* [2007] (FAOSTAT) in developed countries and from *Yevich and Logan* [2003] in developing countries. The switch from fossil fuels as the predominant present-day fuel to wood in preindustrial times was considered in developed countries [*U.S. Energy Information Administration*, 2004]. The historical household biofuel use for developing countries was estimated from the product of the per capita usage and the population change [*United Nations*, 1973]. Biofuel used as agroindustrial fuel (i.e., the use of crop wastes for an energy source in factories) was related to the crop production changes from the FAOSTAT. The emission factors compiled by *Andreae and Merlet* [2001] were used to convert the carbon emissions to O_3 precursors. The ED2 data set has been used for present-day simulations for O_3 precursors by *Ito et al.* [2007b] and for black carbon by *Rotstayn et al.* [2007]. They found good agreement between the model and measurements, which provided some measure of validation for the estimated emissions from BB for the present-day.

[20] The third BB data set (ED3) was that of *Mouillot et al.* [2006] for open biomass burning emissions. The annual emissions on a $1^\circ \times 1^\circ$ grid from 1900 to 2000 were estimated from a global fire map [*Mouillot and Field*, 2005] and carbon cycle model, the Carnegie-Ames-Standord-Approach (CASA) [*Potter et al.*, 1993]. *Mouillot and Field* [2005] estimated that burned area in the United States was 10 times higher at the beginning of the century than in the 1990s, while *Mouillot et al.* [2006] estimated that carbon emissions were only 3 times higher, because their biogeochemical model lowered available biomass as a response to fires. Their estimate of 270–410 Tg C a^{-1} in 1900 was near the center of the 250–610 Tg C a^{-1} range found by *Leenhouts* [1998] under presettlement conditions in the United States. We used the emission factors compiled by *Andreae and Merlet* [2001] and the CASA biome scheme map derived from the MODIS vegetation map [*Friedl et al.*, 2002] by *van der Werf et al.* [2006] to convert the carbon emissions to the O_3 precursors. The open biomass burning emissions of ED3 are combined with the biofuel burning emissions of ED2. Thus the differences between the two databases are due to the differences in the open biomass burning.

[21] Most modeling studies assume no anthropogenic emissions from fossil fuel and biofuel in the preindustrial period and considered open biomass burning emissions to be only 10% of present-day estimates [e.g., *Crutzen and Zimmermann*, 1991; *Gauss et al.*, 2006]. Thus an additional estimate for emissions in 1890 (ED4) was developed by using the original ED1 inventory, setting biofuel emissions to zero and reducing open biomass burning emissions to only 10% of their present-day values for the 1890 simulations, as in the work by *Crutzen and Zimmermann* [1991].

Table 2. Global Emissions of Trace Gases From Biomass Burning[a]

	1890	1990
	ED1	
SO_2	0.9	2.2
NO_X	3.3	7.6
CO	226	572
SRS[b]	9.7	26.4
FRS[c]	3.6	11.2
CH_3OH	1.2	2.3
HCHO	0	1
CH_3CHO	1	3
	ED2	
SO_2	0.8	2.0
NO_X	3.5	8.7
CO	263	647
SRS	11.1	27
FRS	9.1	22
CH_3OH	2.9	7
HCHO	1.4	3
CH_3CHO	1.6	4
	ED3	
SO_2	0.9	2.0
NO_X	5.3	10.8
CO	303	702
SRS	12.2	28.2
FRS	9.7	23.1
CH_3OH	3.4	8.0
HCHO	1.3	3.0
CH_3CHO	1.8	4.1
	ED4	
SO_2	0.1	2.2
NO_X	0.6	7.6
CO	44	572
SRS	5.4	26.4
FRS	2.5	11.2
CH_3OH	0.2	2.3
HCHO	0.2	1
CH_3CHO	0.7	3

[a]Units are TgS/a for SO_2, TgN/a for NO_x, TgCO/a for CO, and TgC/a for NMVOC.
[b]Slower reacting species (SRS).
[c]Faster reacting species (FRS).

[22] The global annual BB emissions for selected species used in this study are given in Table 2. The total amounts of BB emissions for CO are in good agreement among the three data sets of ED1, ED2, and ED3. Figures 1 and 2 show the spatial distribution of the three emission databases for annual CO emissions (kg a^{-1}) from the open biomass burning and biofuel burning categories, respectively. As cited by *Klein Goldewijk* [2001], most of the land conversion from pristine to managed lands in developed countries in temperate regions occurred in the first and second half of the 19th century, while developing countries in the tropics have converted their lands to pasture and cropland in the second half of the 20th century. The forward emission model of ED3 showed major changes in the regional distribution of emissions from fires as a consequence of the switch between emissions from temperate and boreal forests in early times toward the tropics at the present, while the backward emission models of ED1 and ED2 reflect the situation without any strong O_3 precursor emissions in the temperate and boreal regions. In the southeastern United States for 1890, the open biomass burning of ED3 is significantly larger than the biofuel burning of ED2.

[23] Three different methods for determining the seasonal variations in emissions were used. First, the scaling method [*Sudo et al.*, 2002a] which uses the ATSR fire counts [*Arino and Plummer*, 2001] (SV1) was applied to all of the databases to directly compare the different BB data sets. Then, the effect of seasonal variations in open biomass burning emissions was investigated using the ED2 data set with two different scaling methods. The SV2 scaling method was based on the TOMS data [*Duncan et al.*, 2003; *Ito and Penner*, 2005a]. The total numbers of days of available data per month are used to calculate the weighted monthly averages of TOMS AI data, which correspond to absorbing aerosols ($0.2 < AI$) [*Torres et al.*, 2002]. The calculated monthly averaged AI for the 8 regions defined by *Duncan et al.* [2003] was applied to the ED2 data. The SV3 scaling method was based on Moderate resolution Imaging Spectroradiometer (MODIS) fire product [*Justice et al.*, 2002]. We used the Collection 4, version 3 Terra MODIS monthly Climate Modeling Grid (CMG) fire product at a 0.5° spatial resolution from January 2001 through December 2001 [*Giglio et al.*, 2006]. The method used to produce the seasonal variations is based on the MODIS fire counts for 2001. The monthly emissions of the ED2 and the MODIS fire counts are summed to annual data to calculate the scaling factors for each 1° grid, and then the monthly variations in the ED2 emissions are estimated by adjusting the monthly emissions by the MODIS fire counts at 1° resolution.

[24] *Naik et al.* [2007] estimated the RF due to BB by comparing the radiation fluxes without BB emissions and with those. Since there are significant open biomass burning emissions in the preindustrial period, we calculate the radiation fluxes with BB emissions for SO_2, NO_x, CO, and AVOC using CM3-ED1-SV1 in 1890 and FF in 1990 (CM3-BB-1890) and with FF emissions in 1890 and BB emissions in 1990 (CM3-FF-1890) to investigate the source contributions of BB and FF emissions. The RF is calculated from the differences in the radiative fluxes between the 1890 and 1990 simulations. Since the computed forcing values are subject to the effect of nonlinearities in the O_3 chemistry, the sum of BB and FF RF exceeded the total RF from CM3-ED1-SV1. Thus we calculate the proportions of the RF changes due to BB and FF sources for O_3 precursors to its sum of RF, and multiplied those by the total RF from CM3-ED1-SV1.

4. Model Results and Discussion

[25] In this section, we assess the changes in tropospheric O_3 and its RF in response to different AVOC chemical mechanisms and BB emissions with the condensed chemistry. The total RF in the area-weighted mean value is calculated for each simulation and the spatial distributions for the monthly averaged O_3 and its RF are compared below.

4.1. Comparison Between Different Chemical Mechanisms

[26] We perform three sensitivity simulations that provide a quantitative estimate of the O_3 concentration changes resulting from different AVOC chemistry. Here, we first

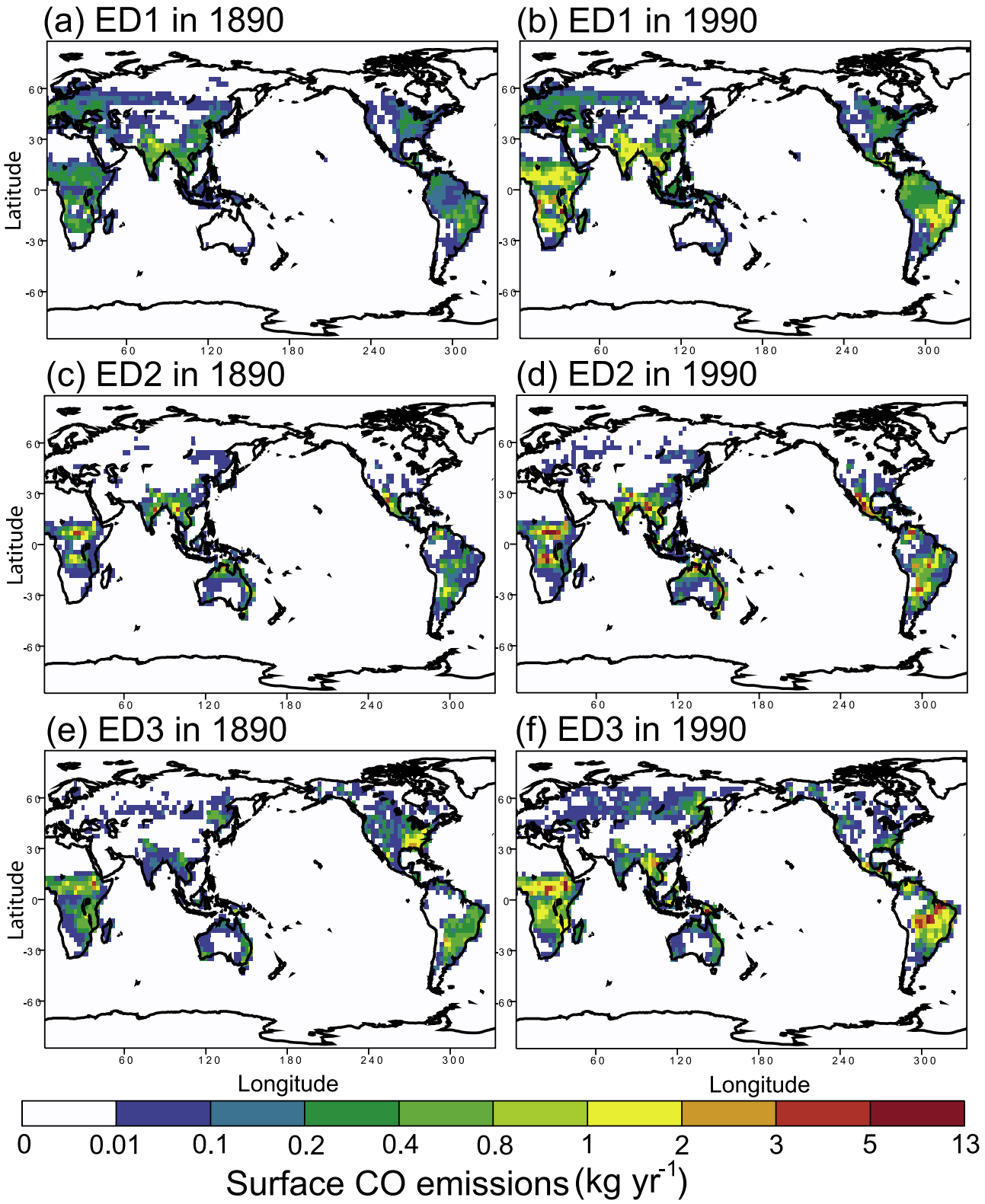

Figure 1. Spatial distribution of the three emission databases of ED1, ED2, and ED3 for annual CO emissions (kg a^{-1}) from open biomass burning in 1890 and 1990.

show the model results for the O_3 concentrations using the default case (CM1-ED1-SV1), and then compare the simulations using the extended chemical mechanism (CM3) to calculations using the default chemical mechanism (CM1) and the simplified photochemistry (CM3) using the ED1 data set.

[27] Figure 3 shows the geographical distribution of surface O_3 concentrations from the simulations of CM1-

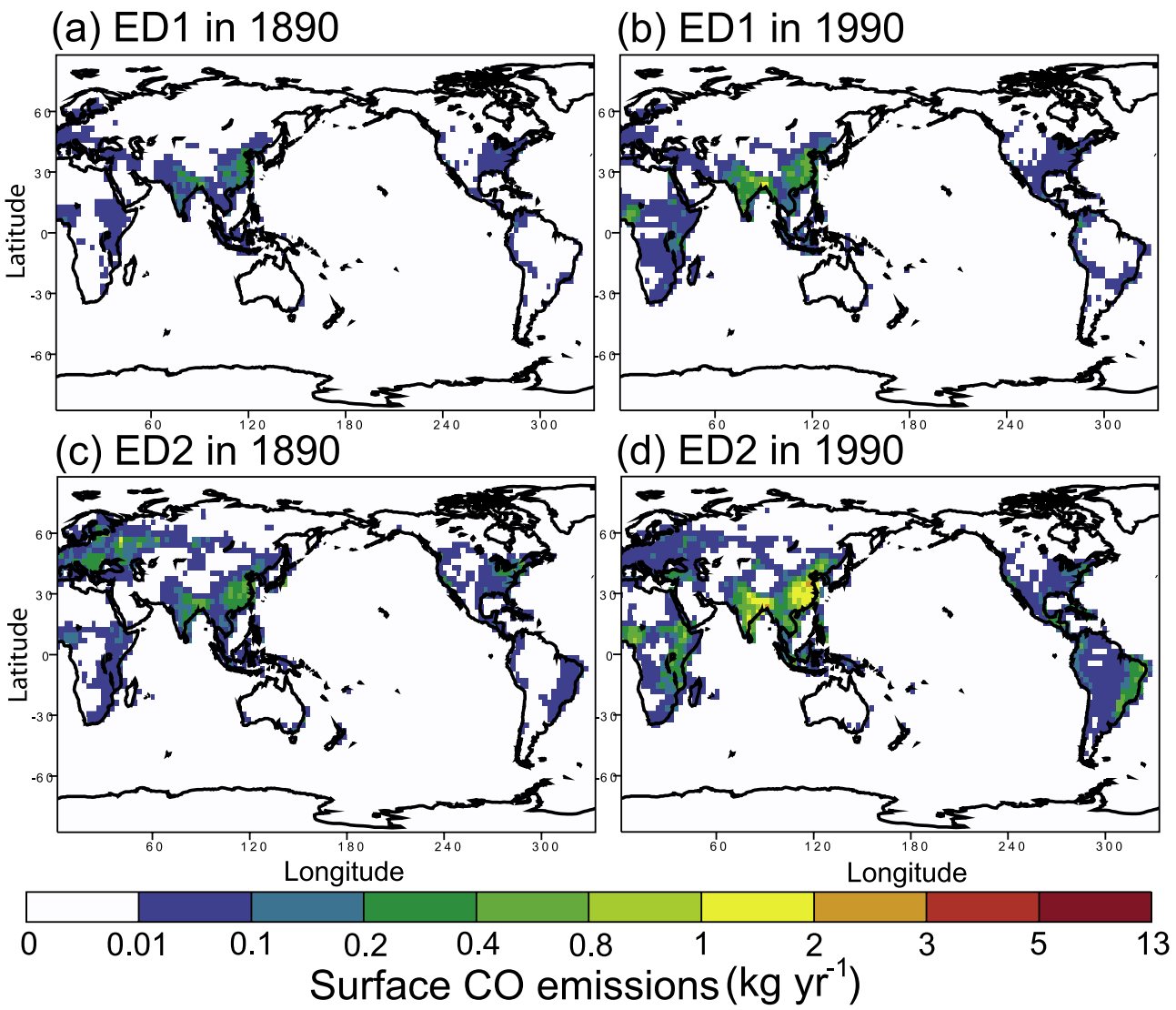

Figure 2. Spatial distribution of the two emission databases of ED1 and ED2 for annual CO emissions (kg a^{-1}) from biofuel burning in 1890 and 1990.

ED1-SV1 in 1890 and 1990. In 1890, the O_3 concentration was 20–30 ppbv over the United States and Europe in August. In 1990, the O_3 concentration was 60–80 ppbv over tropical America and Africa in August.

[28] Figure 4 shows the differences in surface O_3 concentrations with different chemical mechanisms compared to those from CM2-ED1-SV1 in 1990. The differences in O_3 concentrations between the different chemical mechanisms are within 5 ppbv over most locations except between CM1-ED1-SV1 and CM2-ED1-SV1 at near-surface elevations over Eastern Europe, China, and United States during winter, when emission rates for biogenic VOC were low.

[29] The use of the most efficient simplified chemical scheme of CM3 is acceptable for global scale simulations of the radiative effects of tropospheric O_3 changes in a CCM, since the differences between the CM2 and CM3 simulations are small, compared to differences found between different model results [*Stevenson et al.*, 2006] and the different BB databases discussed below. The simulation using CM3 reduces the computation time from that using the CM2 by a factor of 5.2 and from that using CM1 by 1.3. Thus the CCM model with the CM3 mechanism was implemented below to calculate the O_3 and its RF associated with the four different BB data sets and the three different temporal variations using the ED2 data set.

4.2. Atmospheric O_3 Responses Due to Different Biomass Burning Emissions

[30] We focus on the global changes in the distribution of surface O_3 due to the differences in the BB emissions. We first compare the model results for the O_3 concentrations between different BB emissions, and then discuss the differences in the calculated O_3.

[31] Figure 5 shows the differences in surface O_3 concentrations with different emission databases compared to those from CM3-ED1-SV1 in 1890. The results of ED4 are significantly lower than others. Anthropogenic fires existed in the early twentieth century [*Pyne*, 1995]. The fact indicates that the assumption of no anthropogenic BB emissions in preindustrial period needs to be reconsidered.

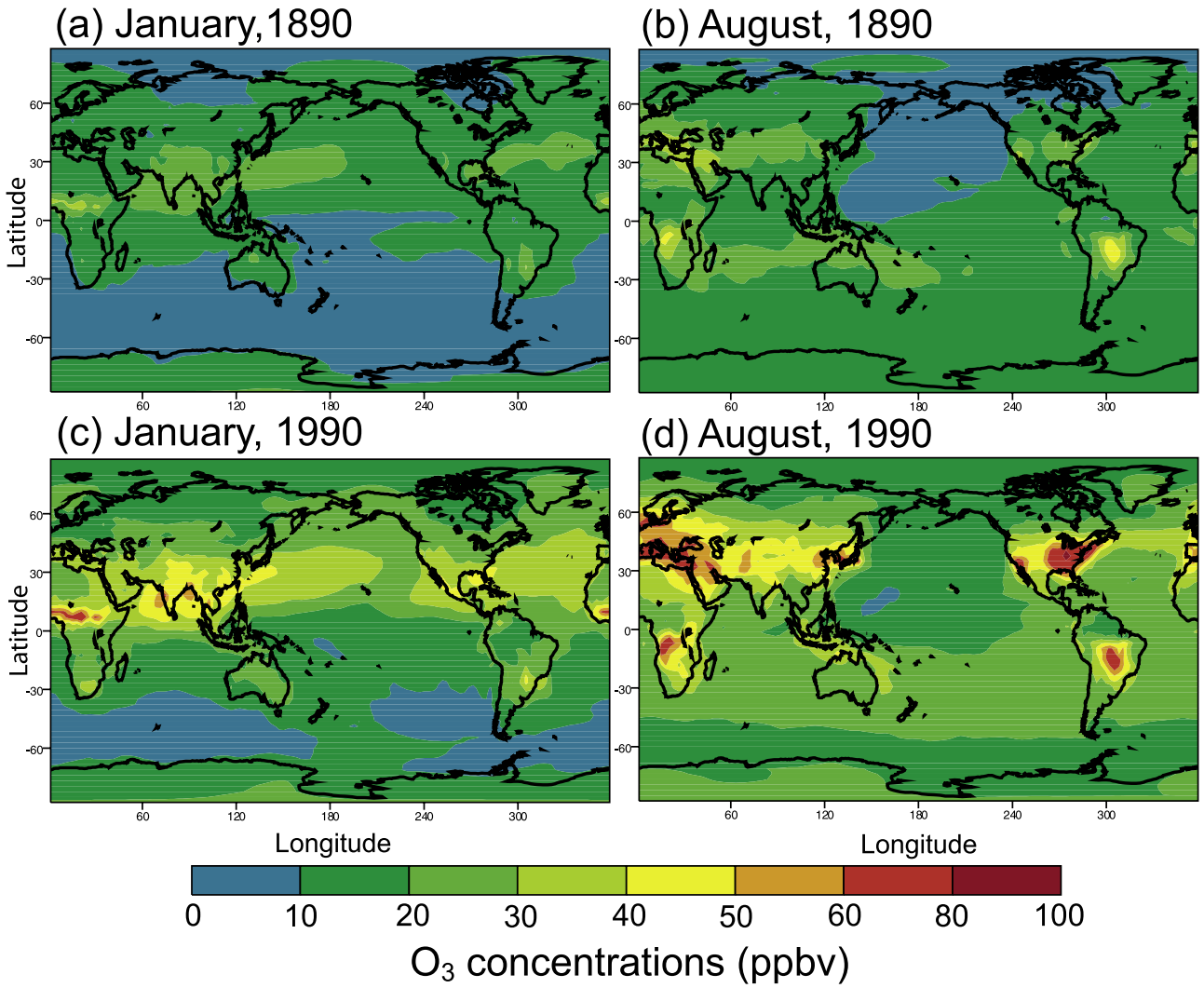

Figure 3. Geographical distribution of surface O_3 concentrations from the CM1-ED1-SV1 simulation in 1890 and 1990.

The ED3 in the southeastern United States yielded high O_3 concentrations of 40–75 ppbv near the surface in August in 1890, while the ED1 and ED2 produced 20–30 ppbv. The fire practices for 1900 in the United States resemble those of contemporary Brazil [*Pyne*, 2001]. This implies that both ED1 and ED2 may underestimate the preindustrial sources of O_3 precursors from BB in the United States. However, the biogeochemical model simulations in ED3 do not include the impacts of settlement and logging practices before 1900 which are certainly important in the United States [*Pyne*, 1982; *Houghton et al.*, 1999]. Improvement in the historical land use changes is required to simulate these human impacts explicitly using spatially disaggregated simulation models [e.g., *McGuire et al.*, 2001; *Jain and Yang*, 2005; *Hurtt et al.*, 2006].

[32] Model validation is a difficult issue because of the scarcity of validation data sets. However, the differences due to the different BB data sets emphasize important scientific issues that remain important subjects for discussion. Figure 6 shows a comparison of the monthly averaged surface O_3 mixing ratio from the model results for 1890 with observations over Tokyo [*Pavelin et al.*, 1999] where the models with different BB data sets exhibit large differences. The simulated preindustrial O_3 concentrations are typically higher than preindustrial surface observations [*Volz and Kley*, 1988; *Marenco et al.*, 1994; *Pavelin et al.*, 1999].

[33] Figure 7 shows the difference between present-day (1990) surface O_3 concentrations with different emission databases compared to those from CM3-ED1-SV1. High surface O_3 concentrations from ED3 data are found over eastern Russia. *Wooster and Zhang* [2004] found that Russian fires burned less fuel and emitted fewer products to the atmosphere because of the surface fires. It is difficult to simulate these regional characteristics using global models, but it could be improved with better treatment of ground versus crown fires in future works. The monthly averages in August calculated from ED3 data are significantly higher than those from ED1 over Brazil. We compare the monthly average surface O_3 concentrations from the sensitivity simulations with different BB emissions in 1990 to ambient measurements at Cuiabá in Brazil [*Logan*, 1999] (Figure 8). This site is strongly affected by BB [*Kirchhoff and Rasmussen*, 1990]. The model systematically overestimates during the wet season,

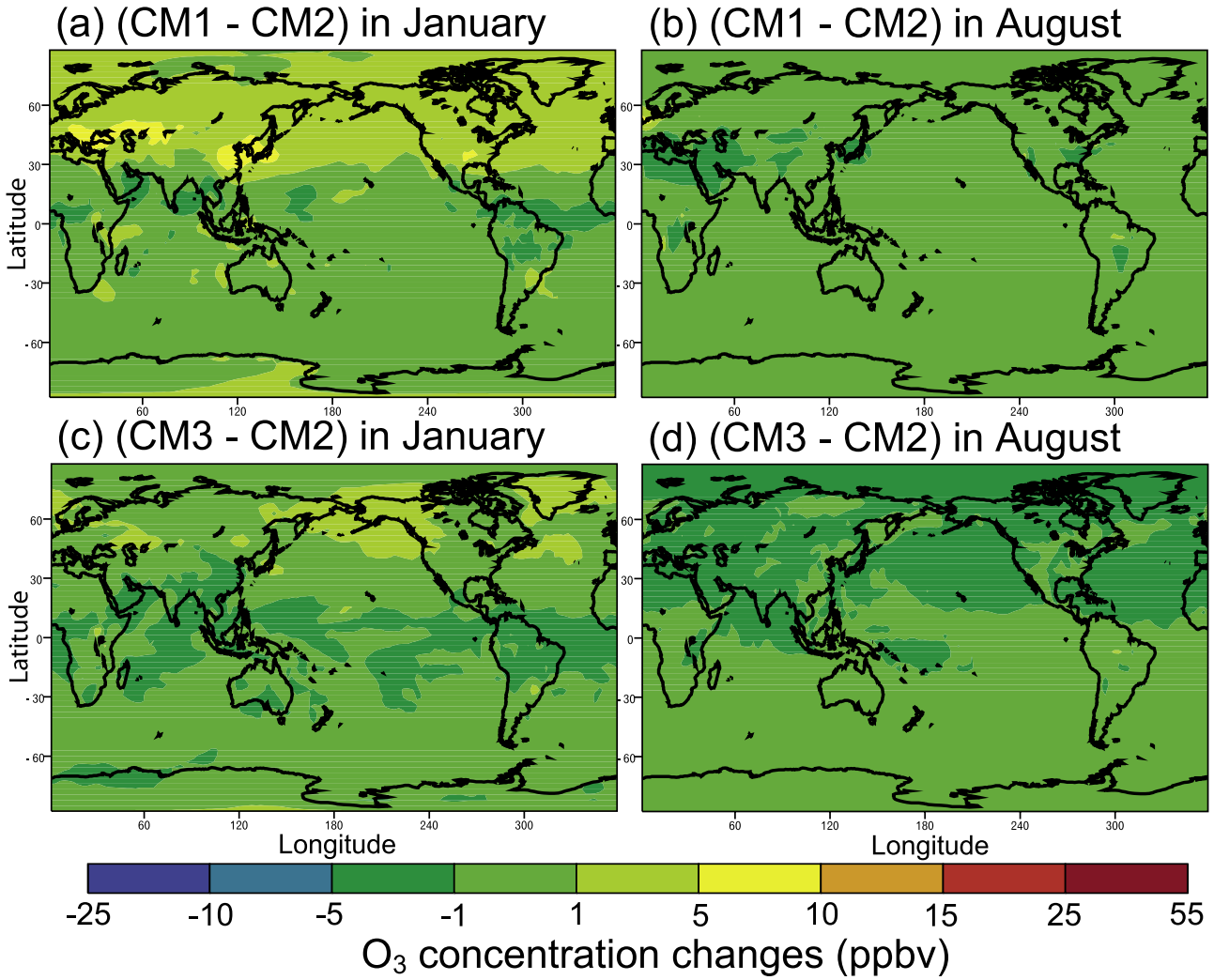

Figure 4. Differences in surface O_3 concentrations with different chemistry mechanisms compared to those from CM2-ED1-SV1 in 1990.

but we focus on the dry season during July, August, and September in this paper. We note, however, that this systematic overestimate was not seen in the IMPACT, which used the CM2 for AVOC but different biogenic VOC emissions and chemistry [*Ito et al.*, 2007b]. The peak O_3 concentration predicted using the ED2 database is in good agreement with the observations. The monthly averages in the burning season calculated from ED1 and ED3 data exceeded 80 ppbv. In terms of the cumulative percentage in the dry season, only 2% of the cases were measured above 80 ppbv in 1987 and 22% in 1988 [*Kirchhoff and Rasmussen*, 1990]. These results suggest that the model results from ED1 and ED3 overestimate the open biomass burning emissions. The peak O_3 concentrations predicted from the seasonal variations of SV1 and SV3 are consistent with the observations, while the SV2 variation peaks earlier than the observations. The correlation coefficient between SV2 and observations for O_3 (0.6) is significantly smaller than others (0.9). These results suggest that finer spatial resolutions are needed to scale the open vegetation burning emissions.

[34] Figure 9 shows the monthly average O_3 concentrations from the simulations with ED1, ED2, and ED3 in comparison with ambient measurements from the field campaigns compiled by *Emmons et al.* [2000], in order to identify whether the changes in the BB emission databases affect the agreement of the vertical profile between models and measurements. The regional differences in O_3 concentrations among the different BB simulations are more pronounced near the surface and less pronounced in the upper troposphere where the radiative balance is sensitive to O_3 changes [*Lacis et al.*, 1990]. Overall, the model results are in good agreement with the observations, although the model with ED3 overestimates O_3 near the surface over eastern Brazil. Even though some of the differences could be due to interannual variability, the interannual variability of O_3 produced by BB over Brazil was rather small for 1979–2000 [*Duncan et al.*, 2003]. The biogeochemical model needs to consider the carbon dynamics associated with land conversions in the Amazon, which includes the decay of biomass left on site, the longer timescale products removed offsite, and the regrowth of secondary forest [e.g.,

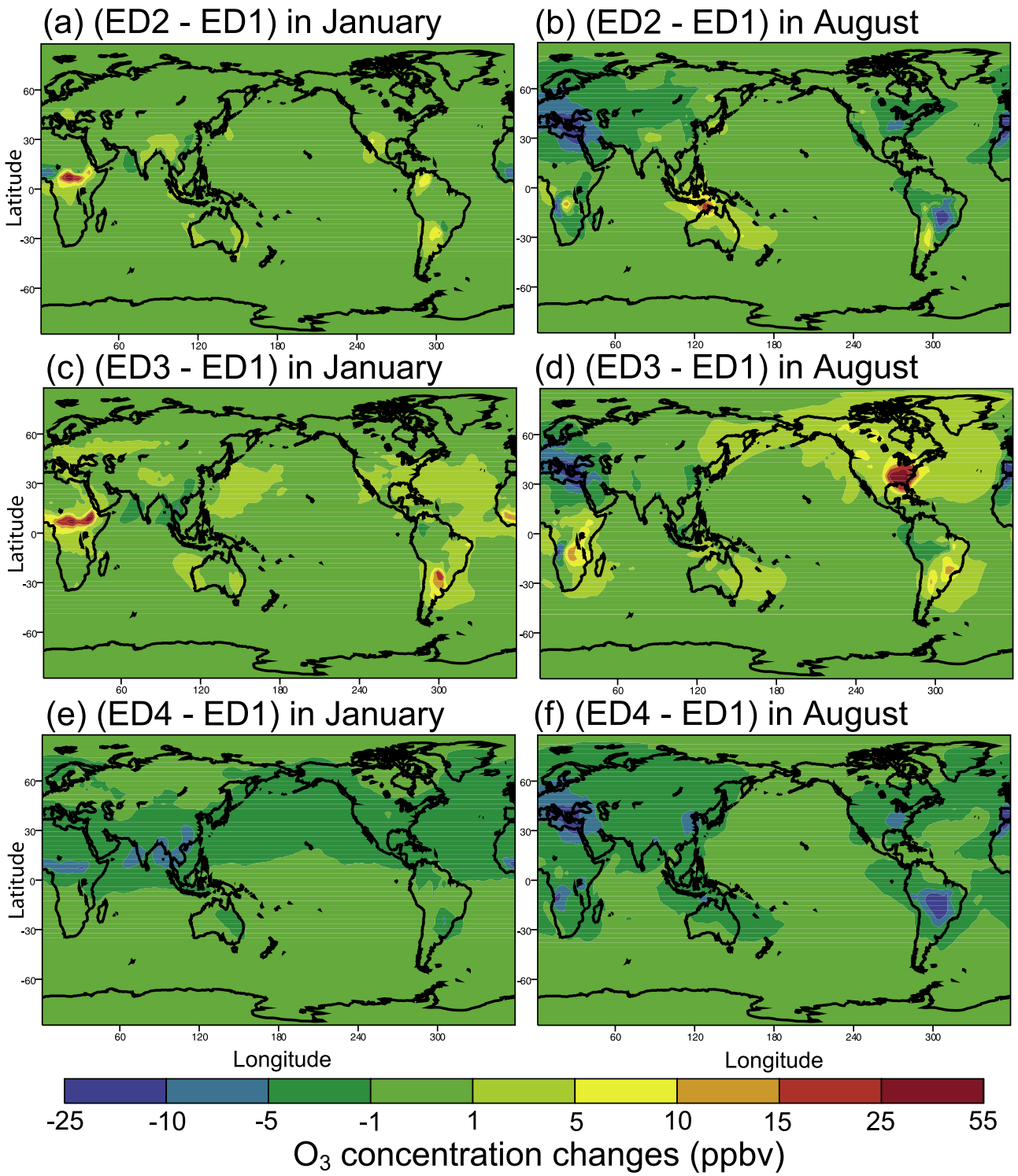

Figure 5. Differences in surface O_3 concentrations with different emission databases compared to those from CM3-ED1-SV1 in 1890.

Guild et al., 1998; *Ramankutty et al.*, 2007]. In southern Africa, ED2 underestimates the surface O_3 concentrations. However, the 1–2 month offset was reported between the peak in hot spot from satellite [*Justice et al.*, 2002] and those in the CO retrievals [*Edwards et al.*, 2006; *Gloudemans et al.*, 2006]. *Ito et al.* [2007a] demonstrated that the characteristic delay between the fire counts and emissions was mainly explained by significant changes in combustion factors for woodlands in their model, based on the measurements [e.g., *Hoffa et al.*, 1999; *Korontzi et al.*, 2003]. Thus it is needed to incorporate the seasonal variations of burned areas with fuel loads, combustion factors, and emission factors at a fine resolution to improve the mismatch between the model results and observations.

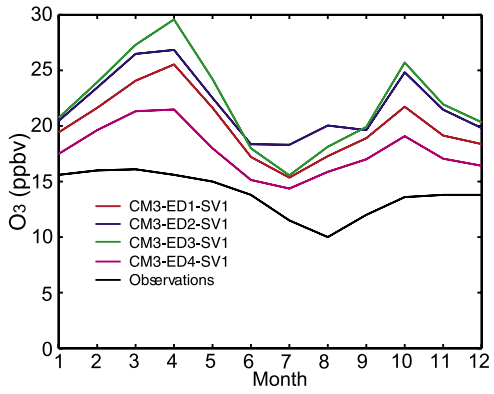

Figure 6. Monthly averaged surface ozone mixing ratio (in ppbv) from the model results for 1890 and observations over Tokyo [*Pavelin et al.*, 1999].

4.3. Contribution of Biomass Burning Emissions to Radiative Forcing Due to O3 Change

[35] We present results from several model experiments to study various aspects of the impact of BB emissions on the RF due to tropospheric O_3 change. The differences in global annual averages of instantaneous RF due to the change in tropospheric O_3 from 1890 to 1990 among three different chemical mechanisms, three different BB data sets of ED1, ED2 and ED3, and three different seasonal variations were insignificant (Table 3). These computed forcing values reflect both BB and fossil fuel (FF) emissions changes. The mean value is identical to the total instantaneous forcing of 0.41 W m^{-2} estimated by *Shindell et al.* [2006] who used the ED1 emission inventory but a different CCM. The global averages of the RF from the ED1, ED2 and ED3 data sets due to tropospheric O_3 increase from 1890 to 1990 were smaller than that calculated with the conventional assumption of ED4 (0.47 W m^{-2}). The difference is comparable to that in the instantaneous forcing and adjusted forcing (e.g., 20% [*Shindell et al.*, 2006]). Fires have been used to clear land for a far longer time [*Pyne*, 1995]. Thus the preindustrial BB emissions need to be considered when evaluating controls on the emissions of trace gases and aerosols for a sustainable society.

[36] The geographical distribution of monthly averaged total instantaneous RF (shortwave + longwave) for January

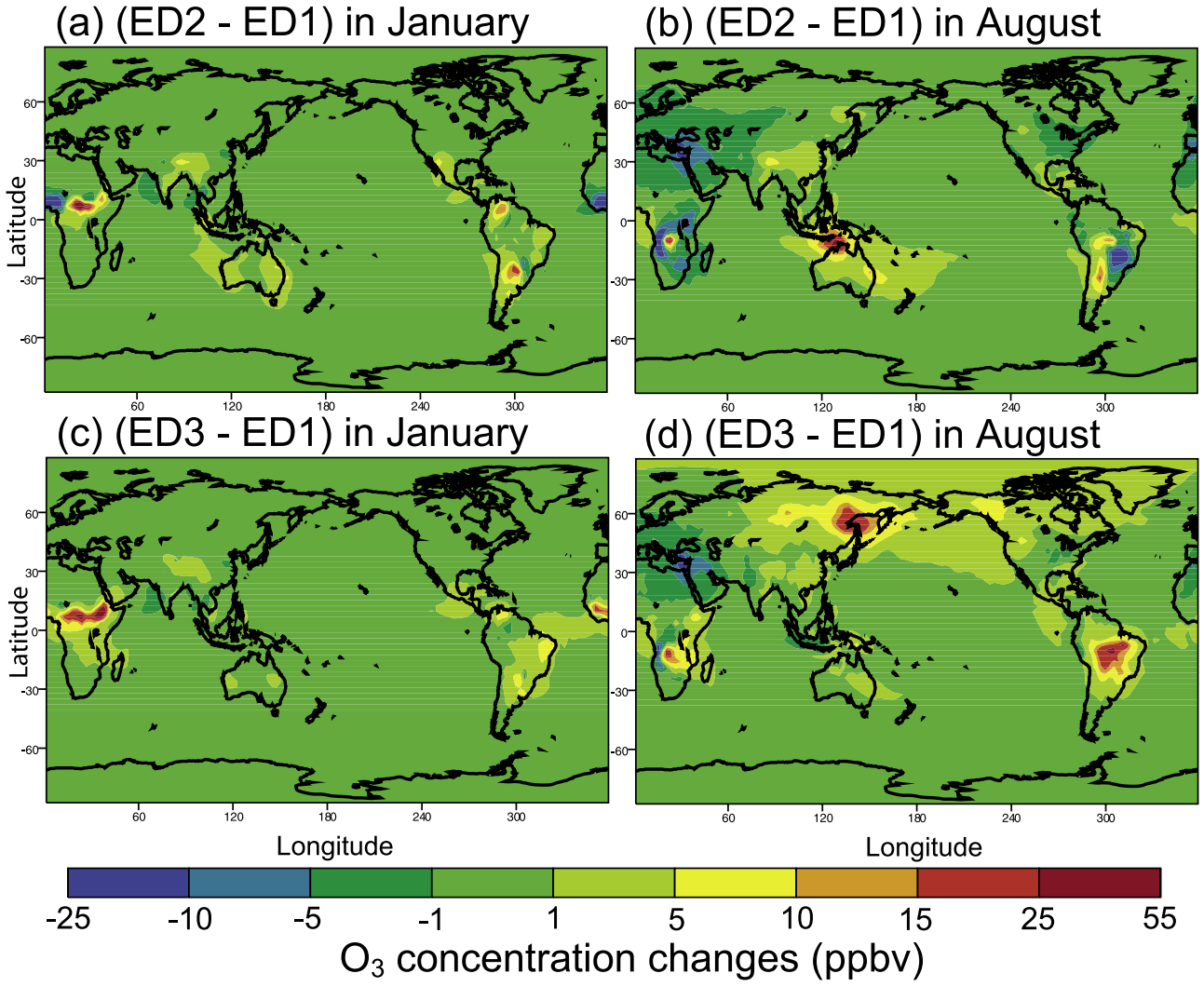

Figure 7. Differences in surface O_3 concentrations with different emission databases compared to those from CM3-ED1-SV1 in 1990.

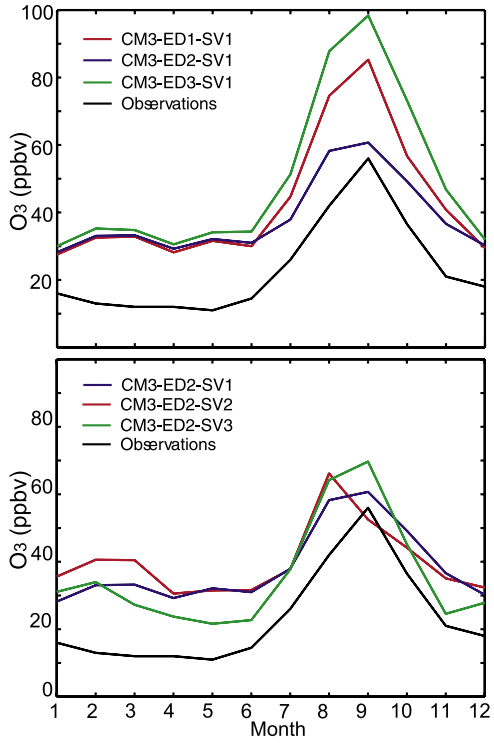

Figure 8. Comparison of monthly average surface O_3 concentrations from the sensitivity simulations with different BB emissions in 1990 with ambient measurements at Cuiabá in Brazil [*Logan*, 1999].

and August from CM3-ED1-SV1 simulation is shown in Figure 10. In January, the total forcing is larger than 0.4 W m^{-2} in the band from 0 to 30 N and larger than 0.2 from 60°S to 60°N. In August, the total forcing is larger than 0.4 W m^{-2} over most of the NH and is stronger than that in January because of the larger O_3 changes and the increased solar irradiance in the NH summer.

Table 3. Radiative Forcing (RF) Due to Tropospheric O_3 Change With Different Simulations Performed in This Study

Name	RF, W m^{-2}
CM1-ED1-SV1	0.42
CM2-ED1-SV1	0.40
CM3-ED1-SV1	0.40
CM3-ED2-SV1	0.42
CM3-ED3-SV1	0.41
CM3-ED2-SV2	0.42
CM3-ED2-SV3	0.42
Mean ± S.D.[a]	0.41 ± 0.01
CM3-ED4-SV1	0.47
CM3-BB-1890	0.15
CM3-FF-1890	0.25

[a]Mean and standard deviations among three different chemical mechanisms, three different BB data sets of ED1, ED2 and ED3, and three different seasonal variations.

[37] Figure 11 shows the difference in the monthly averaged total instantaneous RF (W m^{-2}) (shortwave + longwave) with different emission databases compared to that from the CM3-ED2-SV1 simulation in August. There are significant differences in the southeastern United States and Brazil, where the differences due to different AVOC chemistry and due to different seasonal variations were negligible. The highest preindustrial emission data weakens the regional RF, while the highest present-day data strengthens the regional RF. In Brazil, the monthly averages in August calculated from the highest present-day data set (ED3) exceeds 1.0 W m^{-2}, while the results from the ED1 and ED2 are 0.6–1.0 W m^{-2}. On a global average, this underestimation (ED3) is compensated by lower RF of 1.0–1.4 W m^{-2} in the southeastern United States. In these regions, the forest fires are associated with agricultural usage and land-clearing activities. The backward emission

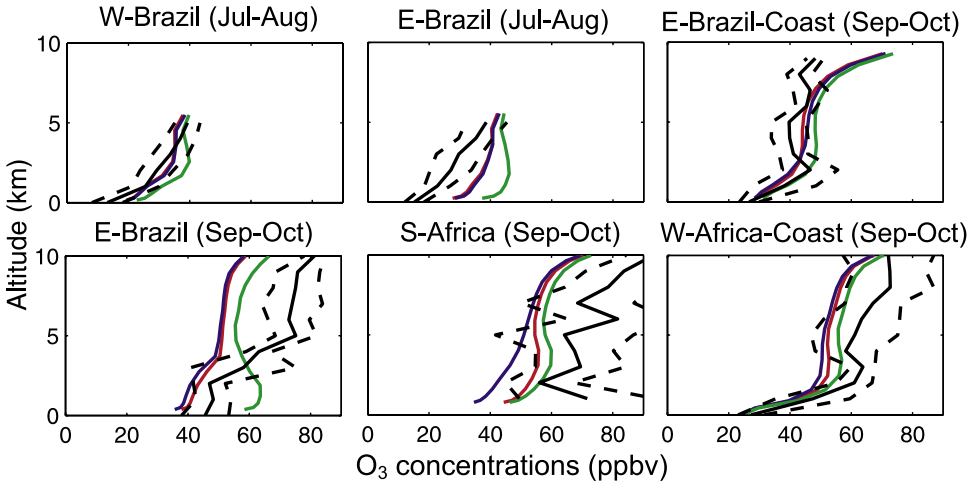

Figure 9. Comparison between measured O_3 in ppb and model results at various sites. The black lines represent the average of measurements over the selected regions and the periods of date reported by *Emmons et al.* [2000]. The black dotted lines show the standard deviations of measured values. The red lines represent the model with CM3-ED1-SV1. The blue lines represent the model with CM3-ED2-SV1. The green lines represent the model with CM3-ED3-SV1.

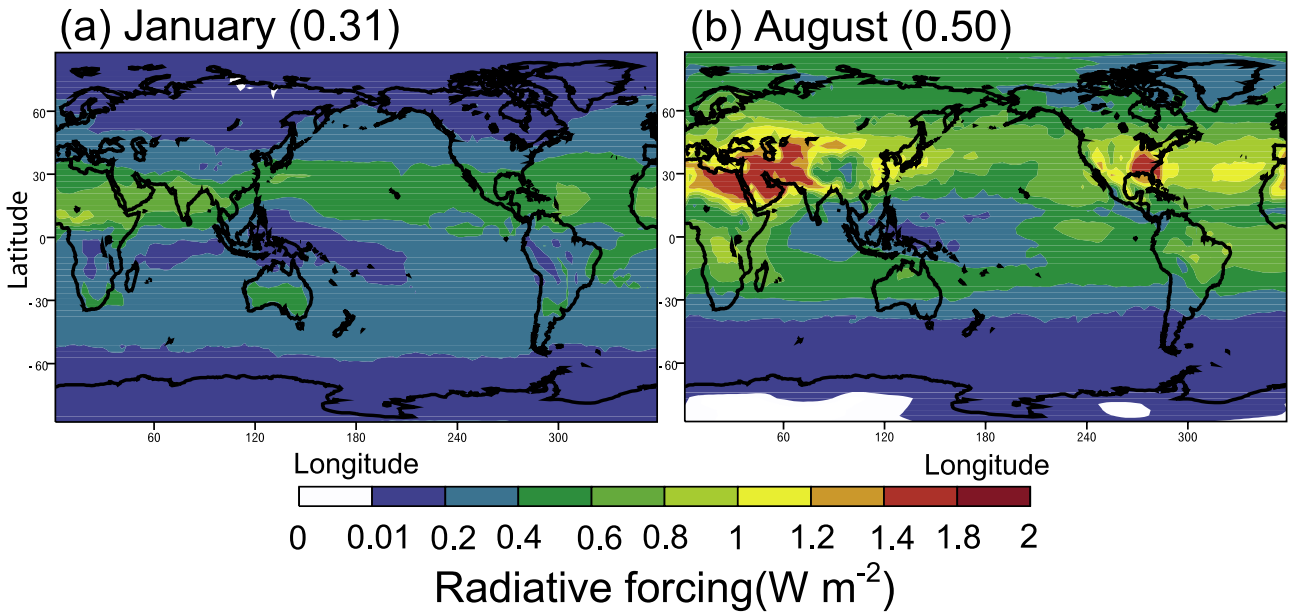

Figure 10. Geographical distribution of monthly averaged total instantaneous radiative forcing (W m^{-2}) (shortwave + longwave) from the CM3-ED1-SV1 simulation. The parentheses represent the global mean RF (W m^{-2}).

models of ED1 and ED2 did not take into account the land conversion in temperate and boreal regions, where fire practices were spatially different from current forest fires [*Pyne*, 1982; *Houghton et al.*, 1999]. The historical changes in the regional emissions may be represented by the forward emission model of ED3, but it requires further studies to represent the present-day O_3 observations near BB sources.

[38] Since the backward emission model results from ED1 and ED2 are in better agreement with the present-day observations for regions downwind of BB sources and the differences in RF between ED1 and ED2 are insignificant, the ED 1 emissions are used for the simulations to investigate the source contributions of BB and FF emissions. Figure 12 shows the monthly averaged total instantaneous RF (W m^{-2}) (shortwave + longwave) due to BB (CM3-BB-1890) and FF (CM3-FF-1890) emission changes for January and August. The impact of BB on the RF is dominant over strong source regions in January. We calculate the global mean total sky BB RF of 0.15 W m^{-2} due to tropospheric O_3 changes from 1890 to 1990. *Naik et al.*

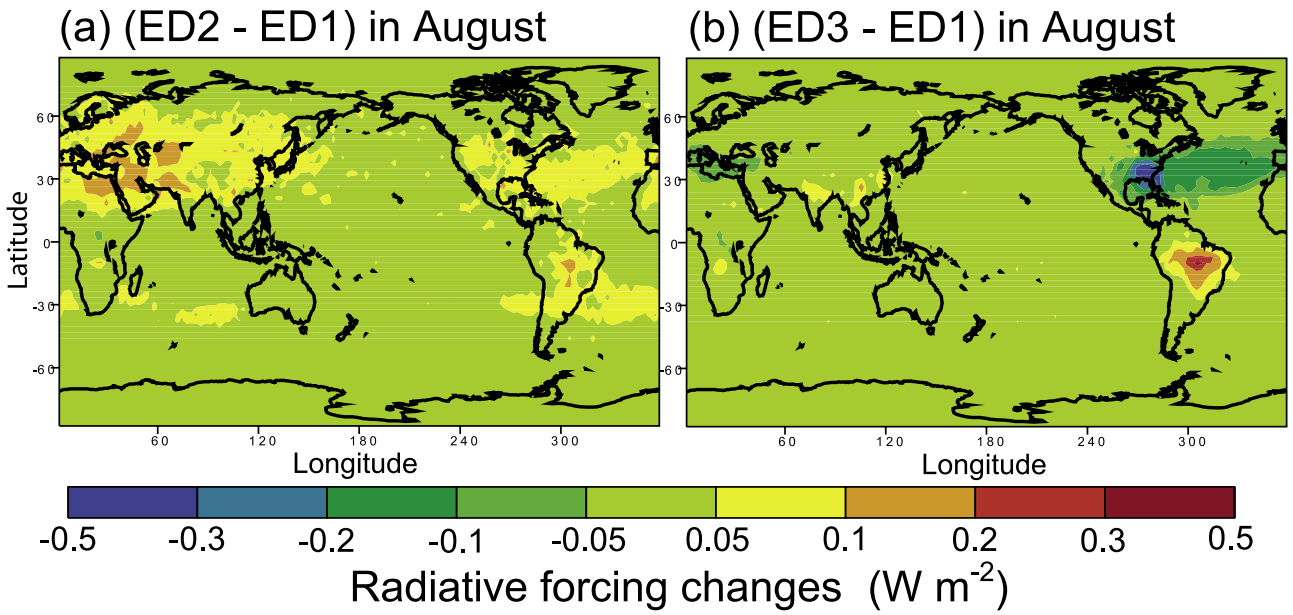

Figure 11. Differences in the monthly averaged total instantaneous radiative forcing (W m^{-2}) (shortwave + longwave) with different emission databases compared to that from CM3-ED2-SV1 simulation in August.

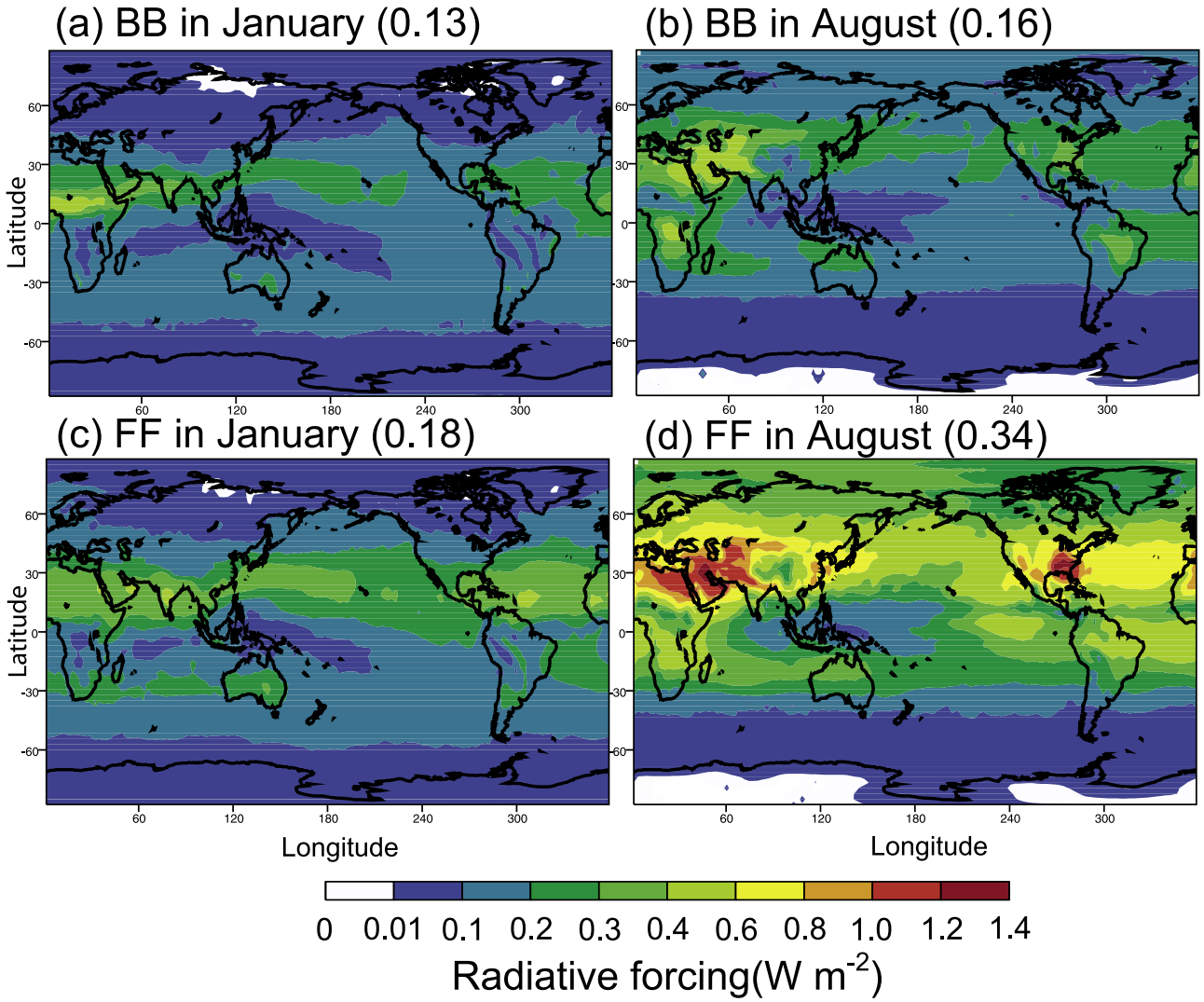

Figure 12. Monthly averaged total instantaneous radiative forcing (W m^{-2}) (shortwave + longwave) from the biomass burning (CM3-BB-1890) emission changes for (a) January and (b) August and the fossil fuel (CM3-FF-1890) for (c) January and (d) August. The parentheses represent the global mean RF (W m^{-2}).

[2007] estimated the adjusted forcing of 0.11 W m^{-2} due to O_3 produced exclusively from BB emissions.

5. Conclusions

[39] Ozone formation in biomass burning plumes has a considerable impact on the regional O_3 concentration during the biomass burning period. Overall, the model results for O_3 concentrations are in good agreement with the present-day measurements at sites that are strongly influenced by BB. However, the results using the ED3 overestimated the surface O_3 observations over Brazil.

[40] The calculated RF among the simulations from three different chemical mechanisms, three different BB data sets of ED1, ED2 and ED3, and three different seasonal variations due to tropospheric O_3 increase from 1890 to 1990 was 0.41 ± 0.01 W m^{-2} on a global average. The radiative effect of an increasing O_3 burden in the troposphere as a result of a 10% open biomass burning emissions reduction from their present-day values for the 1890 simulations [*Crutzen and Zimmermann*, 1991] is nonnegligible (18%), which is comparable to the difference in the instantaneous forcing and adjusted forcing of O_3 [*Shindell et al.*, 2006]. Our computed BB forcing value due to the O_3 changes in the twentieth was 0.15 W m^{-2}. The preindustrial BB emissions need to be improved when evaluating controls on the emissions of trace gases and aerosols for a sustainable society.

[41] The highest preindustrial emission data weakens the regional RF over the southeastern United States, while the highest present-day data strengthens the regional RF over Brazil. In these regions, the most common land uses in the forests are logging and conversion of primary or secondary forests to cattle pasture or shifting cultivation. Biogeochemical models need to consider long-term dynamics of carbon and nutrients due to land use change, which includes the decay of biomass left on site, the longer timescale products removed offsite, and the regrowth of secondary forest [e.g.,

Guild et al., 1998; *Ramankutty et al.*, 2007]. Improvement in the data sets of historical land use changes is required to improve the process-based simulation of historical terrestrial carbon [e.g., *McGuire et al.*, 2001; *Jain and Yang*, 2005; *Hurtt et al.*, 2006]. Further, fuel loads consumed by open fires must be separated from biomass used for fuels because of different emission factors, and these human practices must be treated as subgrid-scale phenomena [*Ito et al.*, 2007a]. Clearly, further studies are needed to refine our understanding of the land cover dynamics on a regional basis.

[42] **Acknowledgments.** We wish to thank F. Mouillot and the Netherlands Environmental Assessment Agency, Netherlands, for kindly providing the emission data sets.

References

Andreae, M. O., and P. J. Crutzen (1997), Atmospheric aerosols: Biogeochemical sources and role in atmospheric chemistry, *Science*, *276*, 1052–1058.

Andreae, M. O., and A. Gelencser (2006), Black carbon or brown carbon? The nature of light-absorbing carbonaceous aerosols, *Atmos. Chem. Phys.*, *6*, 3131–3148.

Andreae, M. O., and P. Merlet (2001), Emission of trace gases and aerosols from biomass burning, *Global Biogeochem. Cycles*, *15*, 955–966.

Arellano, A. F., Jr., P. S. Kasibhatla, L. Giglio, G. R. van der Werf, and J. T. Randerson (2004), Top-down estimates of global CO sources using MOPITT measurements, *Geophys. Res. Lett.*, *31*, L01104, doi:10.1029/2003GL018609.

Arino, O., and S. Plummer (2001), *Along Track Scanning Radiometer World Fire Atlas: Validation of the 1997–98 Active Fire Product*, ESA-ESRIN, Frascati, Italy.

Berntsen, T. K., J. S. Fuglestvedt, M. M. Joshi, K. P. Shine, N. Stuber, M. Ponater, R. Sausen, D. A. Hauglustaine, and L. Li (2005), Climate response to regional emissions of ozone precursors: Sensitivities and warming potentials, *Tellus, Ser. B*, *57*, 283–304.

Bertschi, I., R. J. Yokelson, D. E. Ward, R. E. Babbitt, R. A. Susott, J. G. Goode, and W. M. Hao (2003), Trace gas and particle emissions from fires in large diameter and belowground biomass fuels, *J. Geophys. Res.*, *108*(D13), 8472, doi:10.1029/2002JD002100.

Bey, I., D. Jacob, R. Yantosca, J. Logan, B. Field, A. Fiore, Q. Li, H. Liu, L. Mickley, and M. Schultz (2001), Global modeling of tropospheric chemistry with assimilated meteorology: Model description and evaluation, *J. Geophys. Res.*, *106*(D19), 23,073–23,096.

Boschetti, L., H. D. Eva, P. A. Brivio, and J. M. Grégoire (2004), Lessons to be learned from the comparison of three satellite-derived biomass burning products, *Geophys. Res. Lett.*, *31*, L21501, doi:10.1029/2004GL021229.

Bouwman, A. F., D. S. Lee, W. A. H. Asman, F. J. Dentener, K. W. van der Hoek, and J. G. J. Olivier (1997), A global high-resolution emission inventory for ammonia, *Global Biogeochem. Cycles*, *11*, 561–587.

Brasseur, G. P., D. A. Hauglustaine, S. Walters, P. J. Rasch, J.-F. Müller, C. Granier, and X. X. Tie (1998), MOZART, a global chemical transport model for ozone and related chemical tracers: 1. Model description, *J. Geophys. Res.*, *103*(D21), 28,265–28,290.

Crutzen, P. J., and P. H. Zimmermann (1991), The changing photochemistry of the troposphere, *Tellus, Ser. B*, *43*(4), 136–151.

Crutzen, P. J., L. E. Heidt, J. P. Krasnec, W. H. Pollock, and W. Seiler (1979), Biomass burning as a source of atmospheric gases CO, H_2, N_2O, NO, CH_3Cl and COS, *Nature*, *282*, 253–256.

Dalsøren, S. B., and I. S. A. Isaksen (2006), CTM study of changes in tropospheric hydroxyl distribution 1990–2001 and its impact on methane, *Geophys. Res. Lett.*, *33*, L23811, doi:10.1029/2006GL027295.

Dentener, F., D. Stevenson, J. Cofala, R. Mechler, M. Amann, P. Bergamaschi, F. Raes, and R. Derwent (2005), The impact of air pollutant and methane emission controls on tropospheric ozone and radiative forcing: CTM calculation for the period 1990–2030, *Atmos. Chem. Phys.*, *5*, 1731–1755.

Dlugokencky, E. J., K. A. Masarie, P. M. Lang, and P. P. Tans (1998), Continuing decline in the growth rate of the atmospheric methane burden, *Nature*, *393*, 447–450.

Duncan, B. N., R. V. Martin, A. C. Staudt, R. Yevich, and J. A. Logan (2003), Interannual and seasonal variability of biomass burning emissions constrained by satellite observations, *J. Geophys. Res.*, *108*(D2), 4100, doi:10.1029/2002JD002378.

Edwards, D. P., et al. (2006), Satellite-observed pollution from Southern Hemisphere biomass burning, *J. Geophys. Res.*, *111*, D14312, doi:10.1029/2005JD006655.

Emmons, L. K., D. A. Hauglustaine, J.-F. Müller, M. A. Carroll, G. P. Brasseur, D. Brunner, J. Staehelin, V. Thouret, and A. Marenco (2000), Data composites of airborne observations of tropospheric ozone and its precursors, *J. Geophys. Res.*, *105*, 20,497–20,538.

Etheridge, D. M., L. P. Steele, R. J. Francey, and R. L. Langenfelds (1998), Atmospheric methane between 1000 A.D. and present: Evidence of anthropogenic emissions and climatic variability, *J. Geophys. Res.*, *103*(D13), 15,979–15,994.

Fehsenfeld, F. C., et al. (2006), International Consortium for Atmospheric Research on Transport and Transformation (ICARTT): North America to Europe—Overview of the 2004 summer field study, *J. Geophys. Res.*, *111*, D23S01, doi:10.1029/2006JD007829.

Fiore, A. M., L. W. Horowitz, E. J. Dlugokencky, and J. J. West (2006), Impact of meteorology and emissions on methane trends, 1990–2004, *Geophys. Res. Lett.*, *33*, L12809, doi:10.1029/2006GL026199.

Food and Agricultural Organization (2007), Statistical database, Rome, Italy. (Available at http://www.fao.org/waicent/portal/statistics_en.asp)

Friedl, M. A., et al. (2002), Global land cover mapping from MODIS: Algorithms and early results, *Remote Sens. Environ.*, *83*, 287–302.

Fuglestvedt, J. S., T. K. Berntsen, I. S. A. Isaksen, H. Mao, X.-Z. Liang, and W.-C. Wang (1999), Climatic forcing of nitrogen oxides through the changes in tropospheric ozone and methane; global 3D model studies, *Atmos. Environ.*, *33*, 961–977.

Gauss, M., et al. (2006), Radiative forcing since preindustrial times due to ozone changes in the troposphere and the lower stratosphere, *Atmos. Chem. Phys.*, *6*, 575–599.

Giglio, L., I. Csiszar, and C. O. Justice (2006), Global distribution and seasonality of active fires as observed with the Terra and Aqua Moderate Resolution Imaging Spectroradiometer (MODIS) sensors, *J. Geophys. Res.*, *111*, G02016, doi:10.1029/2005JG000142.

Gloudemans, A. M. S., M. C. Krol, J. F. Meirink, A. T. J. de Laat, G. R. van der Werf, H. Schrijver, M. M. P. van den Broek, and I. Aben (2006), Evidence for long-range transport of carbon monoxide in the Southern Hemisphere from SCIAMACHY observations, *Geophys. Res. Lett.*, *33*, L16807, doi:10.1029/2006GL026804.

Guenther, A., et al. (1995), A global model of natural volatile organic compound emissions, *J. Geophys. Res.*, *100*(D5), 8873–8892.

Guild, L. S., J. B. Kauffman, L. J. Ellingson, D. L. Cummings, E. A. Castro, R. E. Babbitt, and D. E. Ward (1998), Dynamics associated with total aboveground biomass, C, nutrient pools, and biomass burning of primary forest and pasture in Rondônia, Brazil, during SCAR-B, *J. Geophys. Res.*, *103*, 32,091–32,100.

Hansen, J., et al. (2002), Climate forcings in Goddard Institute for Space Studies SI2000 simulations, *J. Geophys. Res.*, *107*(D18), 4347, doi:10.1029/2001JD001143.

Hao, W. M., M.-H. Liu, and P. J. Crutzen (1990), Estimates of annual and regional releases of CO_2 and other trace gases to the atmosphere from fires in the tropics, based on the FAO statistics for the period 1975–1980, in *Fire in the Tropical Biota: Ecosystem Processes and Global Challenges*, edited by J. G. Goldammer, pp. 440–462, Springer, New York.

Herman, J. R., P. K. Bhartia, O. Torres, C. Hsu, C. Seftor, and E. Celarier (1997), Global Distribution of UV-Absorbing Aerosols From Nimbus-7/TOMS Data, *J. Geophys. Res.*, *102*, 16,911–16,922.

Hoffa, E. A., D. E. Ward, W. M. Hao, R. A. Susott, and R. H. Wakimoto (1999), Seasonality of carbon emissions from biomass burning in a Zambian savanna, *J. Geophys. Res.*, *104*, 13,841–13,853.

Houghton, R. A., J. E. Hobbie, J. M. Melillo, B. Moore, B. J. Peterson, G. R. Shaver, and G. M. Woodwell (1983), Changes in the carbon content of terrestrial biota and soils between 1860 and 1980—A net release of CO_2 to the atmosphere, *Ecol. Monogr.*, *53*(3), 235–262.

Houghton, R. A., J. L. Hackler, and K. T. Lawrence (1999), The U.S. carbon budget: Contributions from land-use change, *Science*, *285*, 574–578.

Houweling, S., F. Dentener, and J. Lelieveld (1998), The impact of nonmethane hydrocarbon compounds on tropospheric photochemistry, *J. Geophys. Res.*, *103*, 10,673–10,696.

Hurtt, G. C., S. Frolking, M. G. Fearon, B. Moore, E. Shevliakova, S. Malyshev, S. W. Pacala, and R. A. Houghton (2006), The underpinnings of land-use history: Three centuries of global gridded land-use transitions, wood-harvest activity, and resulting secondary lands, *Global Change Biol.*, *12*, 547–562.

Ito, A., and J. E. Penner (2004), Global estimates of biomass burning emissions based on satellite imagery for the year 2000, *J. Geophys. Res.*, *109*, D14S05, doi:10.1029/2003JD004423.

Ito, A., and J. E. Penner (2005a), Historical emissions of carbonaceous aerosols from biomass and fossil fuel burning for the period 1870–2000, *Global Biogeochem. Cycles*, *19*, GB2028, doi:10.1029/2004GB002374.

Ito, A., and J. E. Penner (2005b), Estimates of CO emissions from open biomass burning in southern Africa for the year 2000, *J. Geophys. Res.*, *110*, D19306, doi:10.1029/2004JD005347.

Ito, A., A. Ito, and H. Akimoto (2007a), Seasonal and interannual variations in CO and BC emissions from open biomass burning in Southern Africa during 1998–2005, *Global Biogeochem. Cycles*, *21*, GB2011, doi:10.1029/2006GB002848.

Ito, A., S. Sillman, and J. E. Penner (2007b), Effects of additional nonmethane volatile organic compounds, organic nitrates, and direct emissions of oxygenated organic species on global tropospheric chemistry, *J. Geophys. Res.*, *112*, D06309, doi:10.1029/2005JD006556.

Jacob, D. J., S. Sillman, J. A. Logan, and S. C. Wofsy (1989), Least independent variables method for simulation of tropospheric ozone, *J. Geophys. Res.*, *94*(D6), 8497–8509.

Jain, A. K., and X. Yang (2005), Modeling the effects of two different land cover change data sets on the carbon stocks of plants and soils in concert with CO_2 and climate change, *Global Biogeochem. Cycles*, *19*, GB2015, doi:10.1029/2004GB002349.

Justice, C. O., L. Giglio, S. Korontzi, J. Owens, J. T. Morisette, D. Roy, J. Descloitres, S. Alleaume, F. Petitcolin, and Y. Kaufman (2002), The MODIS fire products, *Remote Sens. Environ.*, *83*, 244–262.

Kasischke, E. S., J. H. Hewson, B. Stocks, G. van der Werf, and J. Randerson (2003), The use of ATSR active fire counts for estimating relative patterns of biomass burning: A study from the boreal forest region, *Geophys. Res. Lett.*, *30*(18), 1969, doi:10.1029/2003GL017859.

Kawamiya, M., C. Yoshikawa, H. Sato, K. Sudo, S. Watanabe, and T. Matsuno (2005), Development of an integrated earth system model on the Earth Simulator, *J. Earth Simulator*, *4*, 18–30.

Kirchhoff, V. W. J. H., and R. A. Rasmussen (1990), Time variations of CO and ozone concentrations in a region subject to biomass burning, *J. Geophys. Res.*, *95*, 7521–7532.

Klein Goldewijk, K. (2001), Estimating global land use change over the past 300 years: The HYDE database, *Global Biogeochem. Cycles*, *15*(2), 417–433.

Korontzi, S., D. E. Ward, R. A. Susott, R. J. Yokelson, C. O. Justice, P. V. Hobbs, E. A. H. Smithwick, and W. M. Hao (2003), Seasonal variation and ecosystem dependence of emission factors for selected trace gases and PM2.5 for southern African savanna fires, *J. Geophys. Res.*, *108*(D24), 4758, doi:10.1029/2003JD003730.

Lacis, A. A., D. J. Wuebbles, and J. A. Logan (1990), Radiative forcing of climate by changes in the vertical distribution of ozone, *J. Geophys. Res.*, *95*, 9971–9981.

Lamarque, J.-F., P. Hess, L. Emmons, L. Buja, W. Washington, and C. Granier (2005), Tropospheric ozone evolution between 1890 and 1990, *J. Geophys. Res.*, *110*, D08304, doi:10.1029/2004JD005537.

Leenhouts, B. (1998), Assessment of biomass burning in the conterminous United States, *Conserv. Ecol.*, *2*, 1–25.

Liao, H., P. J. Adams, S. H. Chung, J. H. Seinfeld, L. J. Mickley, and D. J. Jacob (2003), Interactions between tropospheric chemistry and aerosols in a unified general circulation model, *J. Geophys. Res.*, *108*(D1), 4001, doi:10.1029/2001JD001260.

Logan, J. A. (1999), An analysis of ozonesonde data for the troposphere: Recommendations for testing 3-D models and development of a gridded climatology for tropospheric ozone, *J. Geophys. Res.*, *104*, 16,115–16,149.

Logan, J. A., J. M. Prather, S. C. Wofsy, and M. B. McElroy (1981), Tropospheric chemistry: A global perspective, *J. Geophys. Res.*, *86*, 7210–7254.

Marenco, A., H. Gouget, P. Nédélec, J.-P. Pagés, and F. Karcher (1994), Evidence of a long-term increase in tropospheric ozone from Pic du Midi data series: Consequences: Positive radiative forcing, *J. Geophys. Res.*, *99*, 16,617–16,632.

McGuire, A. D., et al. (2001), Carbon balance of the terrestrial biosphere in the twentieth century: Analyses of CO_2, climate and land-use effects with four process-based ecosystem models, *Global Biogeochem. Cycles*, *15*(1), 183–206.

Middleton, P., W. R. Stockwell, and W. P. L. Carter (1990), Aggregation and analysis of volatile organic compound emissions for regional modeling, *Atmos. Environ., Part A*, *24*, 1107–1133.

Mouillot, F., and C. B. Field (2005), Fire history and the global carbon budget: A $1^\circ \times 1^\circ$ fire history reconstruction for the 20th century, *Global Change Biol.*, *11*, 398–420.

Mouillot, F., A. Narasimha, Y. Balkanski, J. Lamarque, and C. B. Field (2006), Global carbon emissions from biomass burning in the 20th century, *Geophys. Res. Lett.*, *33*, L01801, doi:10.1029/2005GL024707.

Müller, J.-F. (1992), Geographical distribution and seasonal variation of surface emissions and deposition velocities of atmospheric trace gases, *J. Geophys. Res.*, *97*, 3787–3804.

Müller, J.-F., and G. P. Brasseur (1995), IMAGES: A three-dimensional chemical transport model of the global troposphere, *J. Geophys. Res.*, *100*, 16,445–16,490.

Naik, V., D. Mauzerall, L. Horowitz, M. D. Schwarzkopf, V. Ramaswamy, and M. Oppenheimer (2005), Net radiative forcing due to changes in regional emissions of tropospheric ozone precursors, *J. Geophys. Res.*, *110*, D24306, doi:10.1029/2005JD005908.

Naik, V., D. L. Mauzerall, L. W. Horowitz, M. D. Schwarzkopf, V. Ramaswamy, and M. Oppenheimer (2007), On the sensitivity of radiative forcing from biomass burning aerosols and ozone to emission location, *Geophys. Res. Lett.*, *34*, L03818, doi:10.1029/2006GL028149.

Nakajima, T., and M. Tanaka (1986), Matrix formulations for the transfer of solar-radiation in a plane-parallel scattering atmosphere, *J. Quant. Spectrosc. Radiat. Transfer*, *35*, 13–21.

Nakajima, T., M. Tsukamoto, Y. Tsusima, and A. Numaguchi (1995), Modeling of the radiative process in a AGCM, in *Reports of a New Program for Creative Basic Research Studies, Studies of Global Environment Change With Special Reference to Asia and Pacific Regions*, *Rep. 1–3*, pp. 104–123, Cent. for Clim. Syst. Res., Tokyo.

Olivier, J. G. J., A. F. Bouwman, J. J. M. Berdowksi, C. Veldt, J. P. J. Bloos, A. J. H. Visschedijk, C. W. M. Van der Maas, and P. Y. J. Zandveld (1999), Sectoral emission inventories of greenhouse gases for 1990 on a per country basis as well as on $1^\circ \times 1^\circ$, *Environ. Sci. Policy*, *2*, 241–263.

Page, S. E., F. Siegert, J. O. Rieley, H.-D. V. Boehm, A. Jaya, and S. Limin (2002), The amount of carbon released from peat and forest fires in Indonesia during 1997, *Nature*, *420*, 61–65.

Pavelin, E. G., C. E. Johnson, S. Rughooputh, and R. Toumi (1999), Evaluation of preindustrial surface ozone measurements made using the Schönbein method, *Atmos. Environ.*, *33*, 919–929.

Plass-Dülmer, C., R. Koppmann, M. Ratte, and J. Rudolph (1995), Light non-methane hydrocarbons in seawater, *Global Biogeochem. Cycles*, *9*, 79–100.

Pöschl, U., R. von Kuhlmann, N. Poisson, and P. J. Crutzen (2000), Development and intercomparison of condensed isoprene oxidation mechanisms for global atmospheric modeling, *J. Atmos. Chem.*, *37*, 29–52.

Potter, C. S., J. T. Randerson, C. B. Field, P. A. Matson, P. M. Vitousek, H. A. Mooney, and S. A. Klooster (1993), Terrestrial ecosystem production: A process model based on global satellite and surface data, *Global Biogeochem. Cycles*, *7*(4), 811–842.

Pyne, S. J. (1982), *Fire in America: A Cultural History of Wildland and Rural Fire*, Princeton Univ. Press, Princeton, N. J.

Pyne, S. J. (1995), *World Fire: The Culture of Fire on Earth*, Henry Holt, New York.

Pyne, S. J. (2001), The fires this time, and next, *Science*, *294*, 1005–1006.

Ramankutty, N., H. K. Gibbs, F. Achard, R. DeFries, J. A. Foley, and R. A. Houghton (2007), Challenges to estimating carbon emissions from tropical deforestation, *Global Change Biol.*, *13*, 51–66, doi:10.1111/j.1365-2486.2006.01272.x.

Roelofs, G., and J. Lelieveld (2000), Tropospheric ozone simulation with a chemistry-general circulation model: Influence of higher hydrocarbon chemistry, *J. Geophys. Res.*, *105*(D18), 22,697–22,712.

Rotstayn, L., W. Cai, M. Dix, G. Farquhar, Y. Feng, P. Ginoux, M. Herzog, A. Ito, J. Penner, M. Roderick, and M. Wang (2007), Have Australian rainfall and cloudiness increased due to the remote effects of Asian anthropogenic aerosols?, *J. Geophys. Res.*, *112*, D09202, doi:10.1029/2006JD007712.

Schultz, M. G. (2003), On the use of ATSR fire count data to estimate the seasonal and interannual variability of vegetation fire emissions, *Atmos. Chem. Phys.*, *2*, 387–395.

Shindell, D. T., G. Faluvegi, and N. Bell (2003), Preindustrial-to-present-day radiative forcing by tropospheric ozone from improved simulations with the GISS chemistry-climate GCM, *Atmos. Chem. Phys.*, *3*, 1675–1702.

Shindell, D. T., G. Faluvegi, and L. K. Emmons (2005), Inferring carbon monoxide pollution changes from space-based observations, *J. Geophys. Res.*, *110*, D23303, doi:10.1029/2005JD006132.

Shindell, D., G. Faluvegi, A. Lacis, J. Hansen, R. Ruedy, and E. Aguilar (2006), Role of tropospheric ozone increases in 20th-century climate change, *J. Geophys. Res.*, *111*, D08302, doi:10.1029/2005JD006348.

Sillman, S. (1991), A numerical solution to the equations of tropospheric chemistry based on an analysis of sources and sinks of odd hydrogen, *J. Geophys. Res.*, *96*, 20,735–20,744.

Stern, D. I., and R. K. Kaufmann (1996), Estimates of global anthropogenic methane emissions 1860–1993, *Chemosphere*, *33*(1), 159–176.

Stevenson, D. S., et al. (2006), Multimodel ensemble simulations of present-day and near-future tropospheric ozone, *J. Geophys. Res.*, *111*, D08301, doi:10.1029/2005JD006338.

Sudo, K., and H. Akimoto (2007), Global source attribution of tropospheric ozone: Long-range transport from various source regions, *J. Geophys. Res.*, *112*, D12302, doi:10.1029/2006JD007992.

Sudo, K., M. Takahashi, J. Kurokawa, and H. Akimoto (2002a), CHASER: A global chemical model of the troposphere 1. Model description, *J. Geophys. Res.*, *107*(D17), 4339, doi:10.1029/2001JD001113.

Sudo, K., M. Takahashi, and H. Akimoto (2002b), CHASER: A global chemical model of the troposphere 2. Model results and evaluation, *J. Geophys. Res.*, *107*(D21), 4586, doi:10.1029/2001JD001114.

Swap, R. J., H. J. Annegarn, J. T. Suttles, M. D. King, S. Platnick, J. L. Privette, and R. J. Scholes (2003), Africa burning: A thematic analysis of the Southern African Regional Science Initiative (SAFARI 2000), *J. Geophys. Res.*, *108*(D13), 8465, doi:10.1029/2003JD003747.

Takemura, T., H. Okamoto, Y. Maruyama, A. Numaguti, A. Higurashi, and T. Nakajima (2000), Global three-dimensional simulation of aerosol optical thickness distribution of various origins, *J. Geophys. Res.*, *105*(D14), 17,853–17,874.

Textor, C., et al. (2007), The effect of harmonized emissions on aerosol properties in global models—An AeroCom experiment, *Atmos. Chem. Phys.*, *7*, 4489–4501.

Thompson, A. M., et al. (2001), Tropical tropospheric ozone and biomass burning, *Science*, *291*, 2128–2132.

Torres, O., P. K. Bhartia, J. R. Herman, A. Sinyuk, P. Ginoux, and B. Holben (2002), A long-term record of aerosol optical depth from TOMS observations and comparison to AERONET measurements, *J. Atmos. Sci.*, *59*(3), 398–413.

United Nations (1973), *The Determinants and Consequences of Population Trends*, vol. 1, New York.

U.S. Energy Information Administration (2004), *Annual Energy Review*, Off. of Energy Markets and End Use, U.S. Dep. of Energy, Washington, D. C.

van Aardenne, J. A., F. J. Dentener, J. G. J. Olivier, C. G. M. Klein Goldewijk, and J. Lelieveld (2001), A $1^\circ \times 1^\circ$ resolution data set of historical anthropogenic trace gas emissions for the period 1890–1990, *Global Biogeochem. Cycles*, *15*, 909–928.

van der Werf, G. R., J. T. Randerson, G. J. Collatz, L. Giglio, P. S. Kasibhatla, A. F. Arellano, S. C. Olsen, and E. S. Kasischke (2004), Continental-scale partitioning of fire emissions during the 1997 to 2001 El Niño/La Niña period, *Science*, *303*, 73–76.

van der Werf, G. R., J. T. Randerson, L. Giglio, G. J. Collatz, P. S. Kasibhatla, and A. F. Arellano Jr. (2006), Interannual variability in global biomass burning emissions from 1997 to 2004, *Atmos. Chem. Phys.*, *6*, 3423–3441.

Volz, A., and D. Kley (1988), Evaluation of the Montsouris series of ozone measurements made in the nineteenth century, *Nature*, *332*, 240–242.

von Kuhlmann, R., M. G. Lawrence, P. J. Crutzen, and P. J. Rasch (2003), A model for studies of tropospheric ozone and nonmethane hydrocarbons: Model description and ozone results, *J. Geophys. Res.*, *108*(D9), 4294, doi:10.1029/2002JD002893.

Wild, O., and M. Prather (2000), Excitation of the primary tropospheric chemical mode in a global three-dimensional model, *J. Geophys. Res.*, *105*(D20), 24,647–24,660.

Wild, O., M. J. Prather, and H. Akimoto (2001), Indirect long-term global radiative cooling from NO_x emissions, *Geophys. Res. Lett.*, *28*(9), 1719–1722.

Wong, S., W. Wang, I. S. A. Isaksen, T. K. Berntsen, and J. K. Sundet (2004), A global climate-chemistry model study of present-day tropospheric chemistry and radiative forcing from changes in tropospheric O_3 since the preindustrial period, *J. Geophys. Res.*, *109*, D11309, doi:10.1029/2003JD003998.

Wooster, M. J., and Y. H. Zhang (2004), Boreal forest fires burn less intensely in Russia than in North America, *Geophys. Res. Lett.*, *31*, L20505, doi:10.1029/2004GL020805.

Yevich, R., and J. A. Logan (2003), Assessment of biofuel use and burning of agricultural waste in the developing world, *Global Biogeochem. Cycles*, *17*(4), 1095, doi:10.1029/2002GB001952.

H. Akimoto, A. Ito, and K. Sudo, Frontier Research Center for Global Change, Japan Agency for Marine-Earth Science and Technology, Yokohama 236-0001, Japan. (akinorii@jamstec.go.jp)

J. E. Penner and S. Sillman, Department of Atmospheric, Oceanic and Space Sciences, University of Michigan, Ann Arbor, MI 48109, USA.